# Characterization of string cavitation in large-scale Diesel nozzles with tapered holes

M. Gavaises,[1,a)] A. Andriotis,[1] D. Papoulias,[1] N. Mitroglou,[1] and A. Theodorakakos[2]
[1]*City University London, Northampton Square, GB-London EC1V 0HB, United Kingdom*
[2]*Fluid Research Co., 49 Laskareos Str., GR-Athens 152 34, Greece*

(Received 8 March 2008; accepted 9 December 2008; published online 21 May 2009)

The cavitation structures formed inside enlarged transparent replicas of tapered Diesel valve covered orifice nozzles have been characterized using high speed imaging visualization. Cavitation images obtained at fixed needle lift and flow rate conditions have revealed that although the conical shape of the converging tapered holes suppresses the formation of geometric cavitation, forming at the entry to the cylindrical injection hole, string cavitation has been found to prevail, particularly at low needle lifts. Computational fluid dynamics simulations have shown that cavitation strings appear in areas where large-scale vortices develop. The vortical structures are mainly formed upstream of the injection holes due to the nonuniform flow distribution and persist also inside them. Cavitation strings have been frequently observed to link adjacent holes while inspection of identical real-size injectors has revealed cavitation erosion sites in the area of string cavitation development. Image postprocessing has allowed estimation of their frequency of appearance, lifetime, and size along the injection hole length, as function of cavitation and Reynolds numbers and needle lift. © *2009 American Institute of Physics*. [DOI: 10.1063/1.3140940]

## I. INTRODUCTION

The subject of vortex cavitation has received great attention in literature, particularly in propellers, hydraulic turbines, and hydrofoils, with relevant studies those of Hsiao *et al.*,[1] Arndt,[2] Arndt,[3] and Hsiao *et al.*[4] among many others. Cavitation is linked with undesirable effects such as sharp reduction in performance, increased noise and vibrations, as well as surface erosion. Fundamental cavitation bubble dynamics theories are also well documented, for example, in Ref. 5. Nonspherical bubble dynamics simulation models have been employed in predicting vortex cavitation in Ref. 1 but so far, such models have not been applied to nozzle flows. A recent review paper on experimental techniques and simulation models for cavitation is reported Ref. 6 still, this study refers to flow environments far from those realized in automotive injector nozzles.

The main differences arises from the nozzle geometric configuration and operating conditions: in fuel injectors huge pressure drops are encountered within very short distances, while the lifetime of the formed vortical structures is usually only a fraction of the injection period; the latter is of the order of 1 ms for typical engine operating conditions. Thus, the formation and development of such vortical structures has only been studied in enlarged nozzle replicas operating under steady-state conditions. Nevertheless, their formation and file time is a rather transient phenomenon, as recently reported in Ref. 7.

Although the theory of formation of vortical structures in separation regions is well documented, for example, Refs. 8 and 9, the complexity of the geometries of production nozzles is one of the main reasons for the insufficient information available in such systems and its link to cavitation. Nevertheless, significant research has been dealing with the flow distribution in Diesel injector nozzles and its effect on the injected fuel spray plumes. Diesel injectors operate at high injection pressure reaching 1800 bars while the fuel is discharged through tiny holes of less than $0.2\times10^{-3}$ m in diameter. Under these conditions, cavitation is expected to be formed due to the local pressure drop taking place at the inlet to the injection holes; relevant publications for real-size Diesel injectors are those of Chaves *et al.*,[10] Badock *et al.*,[11] and Arcoumanis *et al.*[12] while a number of investigations studied the development of cavitation in transparent nozzle replicas, for example, Soteriou *et al.*,[13] Soteriou *et al.*,[14] He and Ruiz,[15] and Kim *et al.*[16] Cavitation can be modified or even eliminated completely through appropriate design of the hole entry rounding and the noncylindrical shape of the holes, as shown by Blessing *et al.*[17] although careful optimization is required for achieving engine exhaust emissions without deterioration in performance.

Cavitation in such nozzles has been identified into two district forms of geometric induced and vortex or string cavitation, according to Afzal *et al.*,[18] Arcoumanis *et al.*,[19] and Roth *et al.*[20] The geometric-induced cavitation becomes gradually a relatively well-studied phenomenon initiating at sharp corners where the pressure may fall below the vapor pressure of the flowing liquid. String or vortex cavitation has been observed in the bulk of the liquid of sac or min sac-type nozzles where the volume available may allow formation of large-scale vortices relative to the nozzle geometry. In nozzle flows, two possible flow separation regions typically exist. These can be realized in Fig. 1. In this figure, the vortical structures are represented by an isosurface of the swirl number, as documented by Jeong *et al.*[21] This is a nondimensional parameter used to locate vortical flow structures,

a)Author to whom correspondence should be addressed.

 

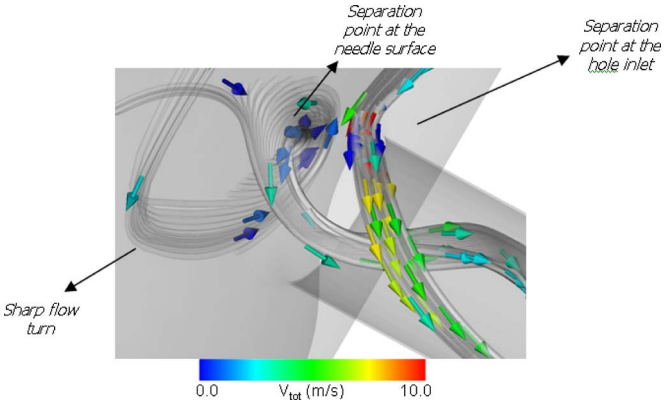


FIG. 1. (Color online) Visualization of flow separation points present in typical Diesel automotive injector nozzles. Velocity vector colored with the magnitude of velocity showing locations of sudden deceleration.

which are shown as transparent tubes in that figure. Inside them, fluid's velocity vectors are indicated. Two distinct structures can be observed. The first one originates from inside the sac volume upstream of the injection hole. As the flow turns in order to enter inside the injection hole, it forms a separation region near the needle seat area and forms a clearly indicated vortex. Flow separation is sometimes associated with formation of cavitation in such locations. As it enters into the nozzle hole passage forms a clearly identified vortex.

The second flow detachment point is located at the top or side surface of the hole inlet. Again, a clear vortical structure can be identified. In addition, a small eccentric placement of the needle valve promotes the asymmetric entrance of the flow in the discharge channels. More recent studies have shown similar behavior in various types of multihole nozzles, as reported by Gavaises *et al.*[22] and Nouri *et al.*[23] Recently, investigations reported in a marine injector by Andriotis *et al.*[7] showed that such structures are found at the core of large-scale recirculation zones developing transiently within the nozzle. However, no evidence for the existence of string cavitation has been reported so far for valve covered orifice (VCO) nozzles, which are known to reduce engine unburned hydrocarbon emissions in modern Diesel engines.

Due to the difficulty in obtaining real-time measurements during the injection process, most of the experimental studies reported refer to experimental devices emulating operating conditions similar to those of Diesel engines. Limited number of studies have shown that dynamic flow similarity based simultaneously on the Reynolds and cavitation numbers (CNs) may allow comparison between the two-phase flow regimes formed in real-size and enlarged nozzle replicas with identical scaled-up geometric characteristics, according to Soteriou *et al.*[24] and Arcoumanis *et al.*[12] In those experiments, Reynolds number (Re) was defined on the basis of hole diameter and mean injection velocity while the CN was defined as $\mathrm{CN}=(P_{\mathrm{inj}}-P_{\mathrm{back}})/(P_{\mathrm{back}}-P_V)$, where $P_{\mathrm{inj}}$, $P_{\mathrm{back}}$, and $P_V$ represent the injection, downstream air, and fluid's vapor pressure, respectively. Although the dynamics of cavitation phenomena at the microscale of bubble dynamics cannot be scaled, experimental evidence suggests that similar flow regimes form macroscopically both in real-size and large-scale injectors. Furthermore, almost all related experimental data show that the discharge coefficient of nozzles with cylindrical holes decreases asymptotically to a minimum value with increasing CN but it is independent of the Reynolds number. Giannadakis *et al.*[25] reported simulations results in real-size and scaled-up models using a variety of cavitation models. Giannadakis *et al.*[25] indeed confirmed that similar flow regimes are formed despite the obvious differences in the microscale level of bubble formation and development. This is effectively an effect of the large number of the cavitation bubbles which coalesce and form the macroscopically observed cavitation cloud. It ought to be mentioned though that no other thorough investigation clarifying issues related to scaling effects in nozzle cavitating flows has been reported so far. Thus, extrapolation of experimental results obtained in large-scale nozzle to real-size injectors, have to be treated with skepticism.

Parallel to the continuing efforts to obtain better experimental information under as realistic conditions as possible, there is an increasing demand for developing and validating computational fluid dynamics (CFD) models able to predict cavitation; relevant publications are those of Schmidt *et al.*,[26] Singhal *et al.*,[27] and Giannadakis.[28] Experimental validation of computational models is essential for assisting to the understanding of the flow processes in complicated nozzle geometries and ultimately, to the design of new nozzle designs. However, the difficulty in manufacturing real-size transparent nozzles that may allow direct visualization of cavitation under realistic conditions imposes simplifications to be made to the design of the nozzle itself and the transient operation of the needle. Complications related to the physical properties and the quality of the working fluid imposes additional difficulties. Nevertheless, experimental data obtained in large-scale injectors can be valuable for the development and validation of cavitation models applicable for fuel injectors. The aforementioned models have been applied so far in simulating the geometric-induced cavitation. Unfortunately, there is no study reported on the prediction of string cavitation in fuel injection equipment. This is mainly due to the lack of experimental data available for the relevant flow phenomena and thus, the incomplete physical understanding of the process.

The present paper aims to provide new experimental data for the origin, formation, area of development and lifetime of the vortex type or string cavitation observed in enlarged replicas of VCO Diesel injector nozzles incorporating tapered (converging) holes. To allow comparison with the majority of previously published studies on cavitation visualization in Diesel injectors, images are compared between identical nozzles incorporating cylindrical holes. The specific design of these nozzles allows for clear optical access to all holes and the nozzle volume to be obtained. High speed images reveal that cavitation strings form not only from cavitation sites inside the injector but also from downstream air trapped to the vortical structures persisting up to the nozzle exit; such observations are made for the first time and reveal the formation of a two-phase flow structure inside Diesel injectors not identified before. Use of CFD simulations has

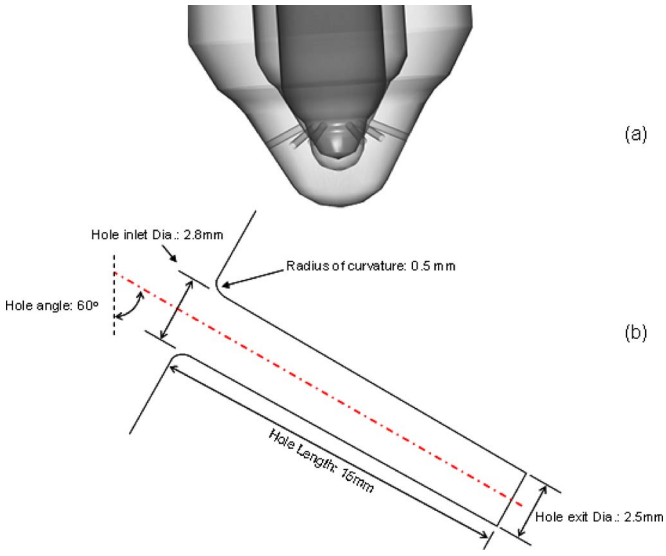


FIG. 2. (Color online) (a) Three-dimensional computer-aided design (CAD) nozzle design and (b) geometry of the injection hole.

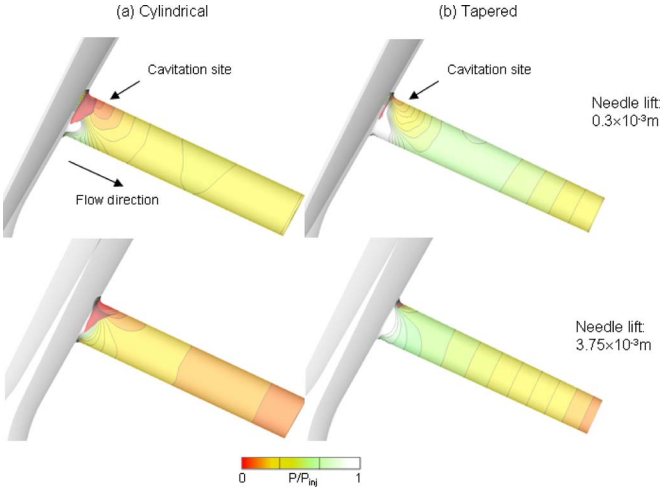


FIG. 3. (Color online) Predicted normalized pressure distribution within the injection of the (a) cylindrical and (b) tapered injection hole at two different needle lifts of $0.3\times10^{-3}$ m (top row) and $1.5\times10^{-3}$ m (bottom row).

provided information about the local flow field at the location where cavitation strings develop and has assisted in the interpretation of the experimental images. Image collection over long enough duration has provided information on the lifetime of cavitation strings and their diameter as function of the flow conditions. Extrapolation though of the present findings to real-size nozzles is not discussed here since such information is not available, neither experimentally nor computationally.

Section II of this paper describes the experimental setup used and the test cases investigated. Then, the various results obtained are presented while the most important findings are summarized at the end.

## II. EXPERIMENTAL SETUP AND TEST CASES

Cavitation visualization has been performed in 15× enlarged transparent nozzle replicas. Transparent nozzles were manufactured from an acrylic transparent material (PERSPEX). The design of the nozzle can be seen in Fig. 2(a); Fig. 2(b) shows a cross section at the symmetry plane of one injection hole. The nozzle itself is a VCO design which implies that the needle valve seals directly in the hole entry area, thus eliminating the dead volume below the injection holes. A recent study by Gavaises *et al.*[29] reported cavitation images and fluid dynamics predictions for two VCO nozzles identical with that used in the present study but with cylindrical holes; emphasis was placed in that study on the effect of two different needle designs which has been found to influence nozzle cavitation and erosion. The present investigation focuses on the shape of the injection holes. The nozzles with tapered holes have shown persistently formation of string cavitation; the images obtained have allowed detailed characterization of this flow structure. The nominal hole diameter is $2.925\times10^{-3}$ m ($0.195\times10^{-3}$ m in the real-size injector). For both designs the radius of curvature at the hole entry has been $\sim0.3\times10^{-3}$ m (approximately $0.2\times10^{-4}$ m in the real-size nozzle). The observed geometric-induced cavitation structures of the cylindrical holes are very similar to those observed in the majority of published data. However, the converging tapered holes greatly modify the pressure distribution within the nozzle, and as a result the formation of cavitation, as can be seen in Figs. 3(a) and 3(b) for the cylindrical and tapered nozzle hole shapes, respectively. Results are presented at $0.3\times10^{-3}$ and $3.75\times10^{-3}$ m, which will be referred to as low and high needle lift positions, respectively; these correspond to $20\times10^{-6}$ and $250\times10^{-6}$ m of equivalent needle lift in the real-size injector, respectively. $P_{inj}$ is the calculated pressure just upstream of the injection hole and $P_{min}$ is the minimum pressure calculated through the simulation. Tapered holes create a smooth pressure gradient along the hole length; the cavitation site is completely eliminated at high needle lift and only a very small region exists for low needle lifts. On the contrary, the computational results obtained for the cylindrical holes indicate a strong cavitation "eye" at the top corner of the injection holes caused by the sharp pressure drop at the hole inlet. The measured and calculated discharge coefficient can be seen in Fig. 4 for the two nozzles and for the two

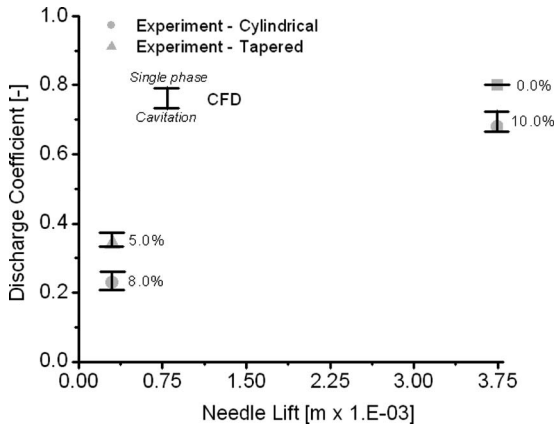


FIG. 4. Measured and predicted nozzle discharge coefficient as function of needle lift.

TABLE I. Operating conditions tested for the large-scale nozzles.

| Needle lift ($\times 10^{-3}$ m) | Pressure (bar) | | Cavitation number | Reynolds number | Equivalent $P_{inj}$ (bar) |
|---|---|---|---|---|---|
| | Inlet | Back | | | |
| 0.3 | 3.75 | 0.75 | 4.1 | 26 000 | 510 |
| 0.3 | 7 | 1.285 | 4.5 | 38 000 | 550 |
| 0.3 | 6.9 | 0.87 | 7.1 | 38 000 | 800 |
| 0.3 | 6.9 | 0.59 | 11.2 | 38 000 | 1200 |
| 1.5 | 6 | 1.1 | 4.5 | 65 000 | 550 |
| 1.5 | 5.9 | 0.52 | 11 | 66 000 | 1200 |
| 3.75 | 5.8 | 0.42 | 13.5 | 71 000 | 1450 |

needle lift sets investigated. The tapered hole nozzles have a much higher discharge coefficient, as expected. In order to keep the fuel injection quantity and injection duration the same between the cylindrical and the tapered holes, the exit diameter of these nozzles was significantly reduced compared to the cylindrical ones, down to $2.43\times10^{-3}$ m ($0.162\times10^{-3}$ m in the real-size injector). On the same plot, predictions from the CFD model are also included; these results are indicated with two horizontal bars. The upper one corresponds to predictions obtained with the single-phase flow solver and they are exhibiting values a little higher than those predicted using the cavitation model of Giannadakis *et al.*[30] This model accounts for the geometric-induced cavitation forming at the hole inlet due to the sharp pressure drop in this area. The model indicates that cavitation may be responsible for up to 5%–10% reduction in the nozzle discharge coefficient at low needle lifts while its relative importance increases with the increased amount of cavitation. This is the case of the cylindrical hole nozzle at the highest needle lift setting. As mentioned, there is no cavitation for the same lift when tapered holes are employed so in this case, only one horizontal bar is depicted. Overall, model predictions are close to the experimental values and thus model predictions can be considered reliable for providing more detailed information of the flow distribution inside the nozzle; more thorough validation of the CFD model used can be found in Ref. 25 and more recently in Ref. 31.

The visualization studies to be reported here provide observations of the flow characteristics in these nozzles which are fundamentally different due to the formation of string cavitation. High speed images have been collected at fixed needle lift positions and various combinations of injection and back pressure values. The steady-state flow test rig that has been described in detail in past studies[20] has been utilized. The working fluid was filtered water at 25 °C controlled by a heater/cooler installed in the storage tank, a degasification filter using membranes was also fitted in the flow rig. The flow rate was controlled by a valve in the pipe downstream of the feed pump and measured by an orifice plate flow meter. Both the injection pressure and the pressure downstream of the injection holes were adjusted by restricting the inflow and outflow of the injector, respectively. In order to reach subatmospheric back pressures and therefore higher CN and Re numbers, a suction pump is installed in addition to the main feed pump. The operating conditions tested for the two large-scale transparent nozzles are summarized in Table I. As can be seen, CNs up to 13.5 have been tested, which are similar to those of the real-size injector operating under engine operating conditions. Imaging was performed for various combinations of the listed parameters. Results to be reported here correspond to three values of needle lift of $0.3\times10^{-3}$, $1.5\times10^{-3}$, and $3.75\times10^{-3}$ m, respectively; these are equivalent to $20\times10^{-6}$, $100\times10^{-6}$, and $250\times10^{-6}$ m in the real-size injector, respectively. The range of Reynolds numbers tested (up to ~71 000) indicates that for the whole range of operating conditions, the fuel flow through the injector nozzles and especially through the holes, is turbulent; laser Doppler velocimetry measurements reported in Ref. 22 for similar operating conditions indicated high levels or rms velocities, attributed not only to liquid turbulence but also to the transient behavior of the formed cavitation structures. It can thus be expected that all flow features behave transiently and with short time scales even at steady-state conditions. Since it is important to gain knowledge about the dynamics of the cavitation inception and formation processes, a high speed digital video system was set up. For the particular cases investigated here, up to 16 000 fps (frames per second) were sufficient to capture the temporal development of cavitation using a shuttering time of 30 ns. Considering that the maximum liquid velocity inside the injection holes is of the order of 30 m/s, during the shuttering time the cavitation bubbles move less than 1 $\mu$m, which can be considered low enough to freeze the image. In total, up to 4000 images have been collected for every case. A strong halogen floodlight together with halogen spotlights were necessary to provide enough light for the intensified charged coupled device video chip in combination with the high frame rates. Following image acquisition, postprocessing has been performed which has provided further insight into the observed two-phase flow structures. Temporal averaging of sufficient number of instantaneous string cavitation images has provided a mean image projected on the two-dimensional (2D) viewing plane, which has been interpreted as the probability of finding vapor within the injection hole. Furthermore, the frequency of appearance of cavitation strings as well as their radius has been derived along the hole length whenever possible. Finally, the limited CFD predictions included to assist in the interpretation of the observed

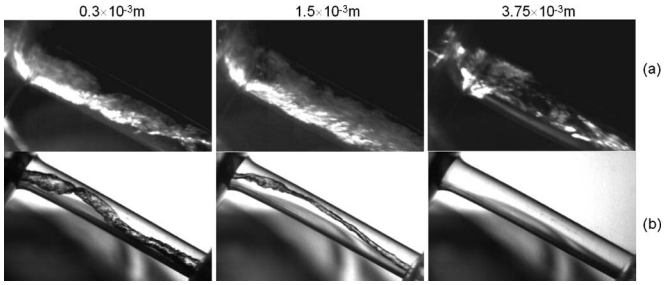


FIG. 5. Sample representative images of cavitation structures formed in the injection hole of the VCO nozzle with grooved needle at three different needle lifts, (a) cylindrical and (b) tapered hole, at the maximum Reynolds and CNs investigated.

cavitation regimes have been obtained with the author's in-house CFD code; details of the specific models and flow processes considered can be found in Ref. 25.

## III. RESULTS AND DISCUSSION

### A. Cavitation regimes

The first findings regarding the cavitation regimes formed inside the cylindrical and tapered nozzle holes can be realized from Fig. 5. This figure shows representative images of the observed cavitation for all three needle lift positions investigated. Clear differences can be observed between the cylindrical and the tapered holes. For the low needle lift case, the cylindrical hole nozzle exhibits mainly the formation of a cavitation cloud at the hole inlet, which occupies most of the hole inlet cross sectional area. The majority of the formed cavitation bubbles seems to collapse within the injection hole before reaching the hole exit. This regime has been referred to in past studies as incipient cavitation, for example, see Ref. 32. Increasing needle lift results to fully developed cavitation, which extends up to the hole exit. In addition to the geometric-induced cavitation, vortex or string cavitation has been observed, similar to that of Roth *et al.*[33] The structure of cavitation is clear inside the tapered nozzle hole. There, string cavitation dominates the flow at low and intermediate lifts while both geometric and string cavitation disappear completely at high needle lifts. This type of cavitation structures has been observed in similar enlarged nozzle designs investigated over the past few years while limited evidence has been also reported in real-size nozzle operating at realistic injection pressures and needle opening/closing events, as reported by Arcoumanis *et al.*,[12] Blessing *et al.*,[17] and Roth *et al.*[33] More recently, in Ref. 22 the flow in a relatively different nozzle geometry used with low-speed two-stroke large Diesel engines was dominated by string cavitation, which was also linked to important effects on the atomization process of the injected liquid.[34] In a complementary study by Andriotis *et al.*,[35] limited information on similar structures of string cavitation have been observed but this time in nozzles incorporating tapered converging holes. It is thus of interest to explore in more detail the conditions which lead to the initiation and area of development of these observed two-phase flow structures.

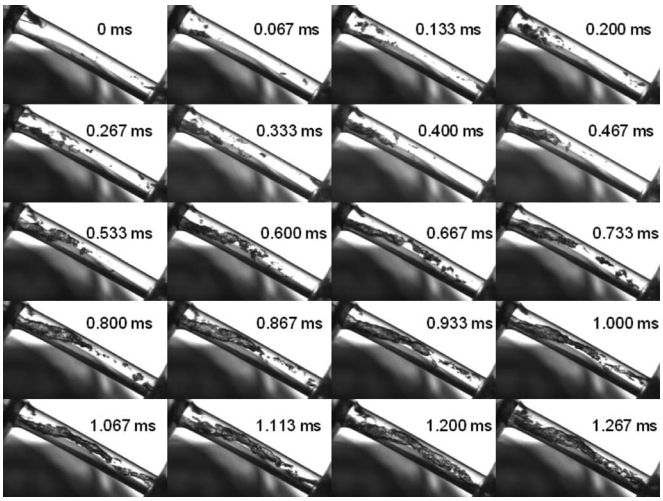


FIG. 6. Sequence of events showing the formation of string cavitation from cavitation bubbles formed at the top corner of the injection holes feeding the vortical structure present inside the injection hole (needle lift: $0.3 \times 10^{-3}$ m, Re=38,000, and CN=11.2).

### B. String cavitation origin

Two questions may arise from Sec. III A: (i) How cavitation strings originate? (ii) Where do they develop? The first one can be answered by observing the following two figures. Figure 6 shows the formation of a cavitation string as captured from the high speed camera at 16 000 fps. For this particular operating condition, a weak geometric-induced cavitation bubble cloud is forming at the top corner of the injection hole. Cavitation bubbles found at locations closer to the axis of symmetry of the injection hole suddenly elongate and may take the shape of the observed strings within only a very small time interval. Figure 7 shows a different origin or mechanism of string cavitation formation observed at the intermediate needle lift of $1.5 \times 10^{-3}$ m. This time, the increased needle lift combined with the tapered hole shape eliminates geometric-induced cavitation sites pre-existing to the formation of string cavitation. Thus, initially, a single-phase liquid flow is present within the injection hole. Despite that, the sequence of high speed images indicates that down-

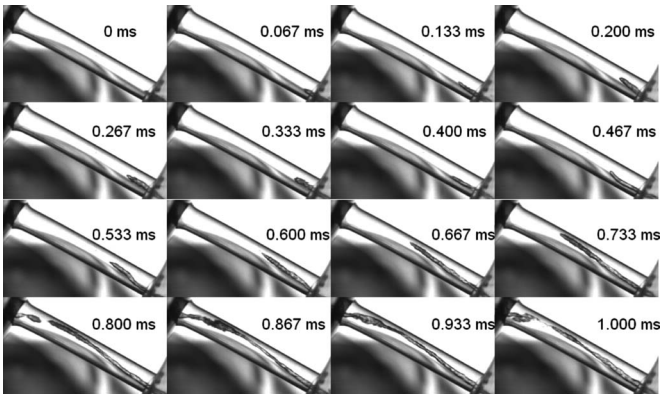


FIG. 7. Sequence of events showing the formation of string cavitation originating from the air downstream of the injection hole and developing upstream inside the injection hole (needle lift: $1.5 \times 10^{-3}$ m, Re=65 000, and CN=4.5).

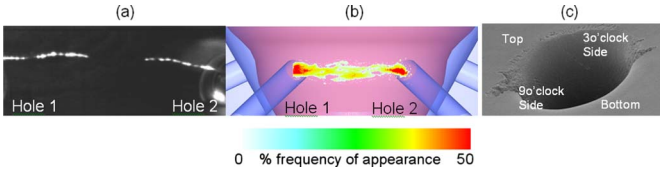


FIG. 8. (Color online) (a) Instantaneous image and (b) time-averaged probability of string cavitation appearance between two adjacent injection holes and (c) SEM image of cavitation erosion at the entry to the injection hole, believed to be caused by string cavitation (from Ref. 29).

stream air may enter into the injection hole and propagate upstream, forming again the observed two-phase flow structure. It is surprising though to observe that flow process, considering that the liquid toward the hole exit has almost an axial velocity component, as all past experimental and computational studies have indicated. Cavitation strings have been observed not only inside the injection hole but also in the space between adjacent injection holes. The image of Fig. 8(a) shows a cavitation string linking two adjacent holes. Averaging of all acquired images results to the picture of Fig. 8(b); this can be interpreted as the probability of finding a cavitation string at a particular location in the space between two adjacent holes. The fact that the maximum levels of the plotted probability is less than 50% makes obvious that strings are not present continuously. In addition, their presence is more pronounced near the hole inlet rather than in the space between the hole inlet and exit. This is due to the mechanism of their formation and further development. As the pressure distribution plotted in Fig. 3 indicates, in the areas of formation of string cavitation the pressure is well above the vapor pressure of the flowing liquid, which is usually considered as the threshold for cavitation inception. Thus, cavitation strings do not form due to the local pressure drop but they rather represent a mechanism of vapor transport in these areas. This transport mechanism sometimes—but not always—results to a cavitation string linking the two adjacent holes. In most cases, two strings are formed, each one originating from the corresponding hole, but disappear before coalescing and forming the continuous stream of vapor linking adjacent holes. This explains the lower levels of the plotted string probability of Fig. 8(b) at the central part of the injector. A scanning electron microscope (SEM) picture of the actual injector reported recently in Ref. 29 and also shown here in Fig. 8(c) indicates that cavitation strings may also be responsible for cavitation erosion. In the absence of flow measurements in the areas of string cavitation development, the predicted flow field has been utilized to provide such evidence. Figure 9 shows predicted stream lines inside the nozzle volume as well as the injection holes for the low needle lift case. The plotted streamlines of Fig. 9(a) are colored according to the swirl number (Jeong *et al.*[21]). It is evident that in the space between the holes, a vortical structure is present. This is formed in the narrow space upstream of the injection holes due to the turning of the upstream flow in its path toward the discharge channels. Similarly, the flow distribution inside the injection hole, shown in more detail in Fig. 9(b), has also a swirling pattern with a vortical structure formed around its central part. This originates from the non-

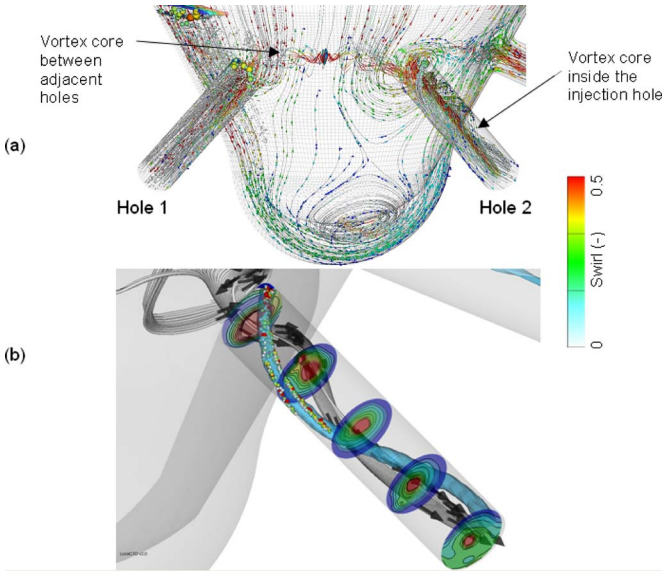


FIG. 9. (Color online) Model predictions for the original VCO nozzle using slightly eccentric needle position. Calculations indicate (a) formation of a strong vortex formed in between adjacent holes and (b) the vortex core inside the injection hole can be linked with the area where string cavitation has been observed.

uniform flow entering into the holes from the 3 and 9 o'clock sides. The observed flow nonuniformity may originate from the nonsymmetric design of the feed fuel pipe; other factors may be a small eccentricity of the needle lift which is known to affect the flow distribution in the narrow space between the needle and the injection holes as well as the transient development of the flow itself. The latter may be attributed to flow turbulence but also to the instantaneous variation of the discharge coefficient of individual injection holes. This can be caused by the formation of the weak geometric cavitation at the top corner, which instantly results to a reduction in the flow rate through that hole, as reported in Ref. 25 and thus, creating a cross flow between adjacent holes. Combination of the observed cavitation strings with the predicted flow vortices developing within the injector indicates that cavitation strings develop in the area of these vortices, effectively they represent a "visualization" of their presence, as supported by the trajectory of cavitation bubbles specifically introduced into the flow and captured at the center of the vortical structure, following closely its path toward the hole exit.

### C. String cavitation characterization

Having identified their origin and area of development, we proceed now to the last set of results which provide information on the temporal and spatial characteristics of string cavitation as function of the operating conditions. With the given experimental rig, the effect of CN, Reynolds number, and needle lift has been evaluated. Figure 10 depicts clearly the expected effect of increasing CN keeping the flow rate through the rig constant and the needle at its lowest lift of $0.3\times10^{-3}$ m. It can be seen that the formed strings are thinner at low CNs while no differences in their shape and extend can be observed with sufficient high CN.

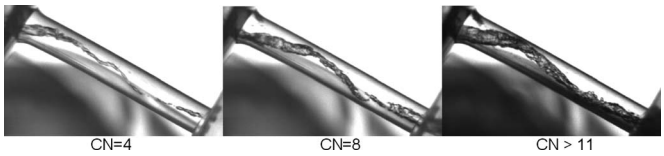


FIG. 10. Effect of CN of string cavitation structure inside the tapered injection hole (needle lift: $0.3\times10^{-3}$ m and Re=38 000).

In an effort to provide a visual representation of the thousand of the collected frames which show the dynamic development of the phenomenon at nominal quasisteady-state flow conditions, Fig. 11 is presented. On the plot, every horizontal line plotted indicates the instantaneous presence of string cavitation in the corresponding location along the injection hole. The color used is according to the local diameter of the string at each location, normalized with the hole diameter. Thus, this graph allows for a convenient representation of the dynamics of string appearance and size for all individual frames collected. The last three plots [Figs. 11(a)–11(c)] indicate that the phenomenon is greatly affected by the CN keeping the same Reynolds number (fixed flow rate). Increasing CN results to more frequent appearance of cavitation strings which gradually occupy the whole injection hole. Larger diameters can be found at the inlet and the exit of the injection hole while strings seem to become thinner and appear less at the central part. Comparison between Figs. 11(a) and 11(b) indicates that the flow rate (Reynolds number) may also be an influential parameter but at low CNs.

From these plots, the percentage of string appearance at a specific location within the injection hole and the temporal mean size has been estimated and shown in Figs. 12(a) and 12(b), respectively. The plots reveal that at the hole inlet, cavitation strings are always present but they disappear as they move inside the injection hole. Toward the hole exit,

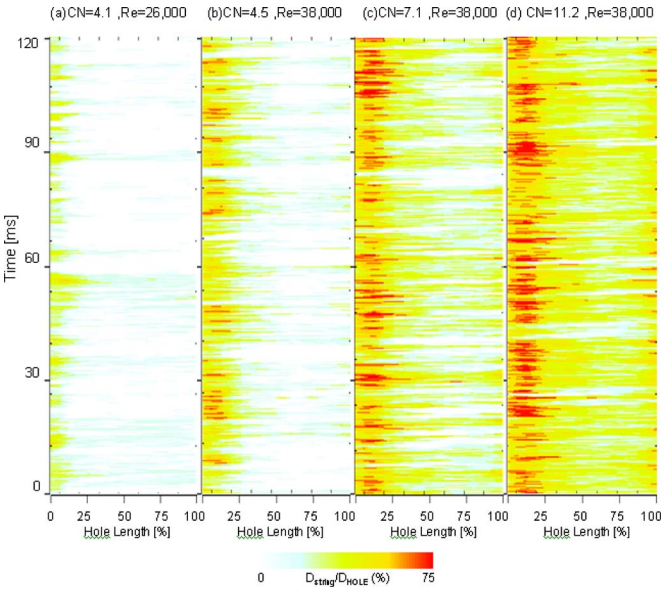


FIG. 11. (Color online) Spatial extent and temporal development of string cavitation inside the injection as function of Reynolds and CNs for $0.3\times10^{-3}$ m needle lift; color according to normalized string diameter.

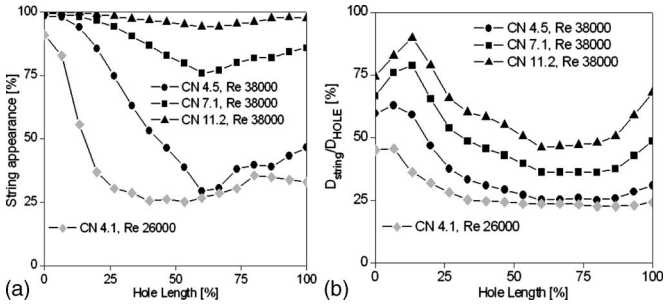


FIG. 12. Effect of Reynolds and CNs on (a) string appearance along the hole length expressed as percentage of time and (b) normalized mean string diameter along the hole length (needle lift: $0.3\times10^{-3}$ m).

string appearance increases again due to their formation from the downstream air, as explained previously. The decrease in their appearance is also linked with a decrease of their size. At the hole inlet, strings may occupy up to 75% of the hole cross sectional area while their size drops to 50% at the central part of the hole. This variation in size is also present even at sufficient high cavitation and Reynolds numbers which correspond to continuous presence of cavitation strings inside the injection hole.

Another visual representation of cavitation strings can be seen in Fig. 13. This plot shows the effect of cavitation and Reynolds numbers on the temporal averaged string presence at a specific location on the 2D viewing plane of the camera, which can be interpreted as the probability of finding a cavitation string at a particular location along the hole length. The images reveal that strings originate mainly from the bottom part of the hole inlet or exit while they follow a path toward the upper part of the central hole region.

All previous results refer to the low needle lift case of $0.3\times10^{-3}$ m. Significant differences have been observed with increasing needle lift. A quantification of these differences between the low and intermediate needle lift cases is presented in the following figures. As already pointed out, the geometric-induced cavitation site is significantly reduced or even eliminated with increasing needle lift for the tapered nozzle hole geometry due to the differences in the pressure

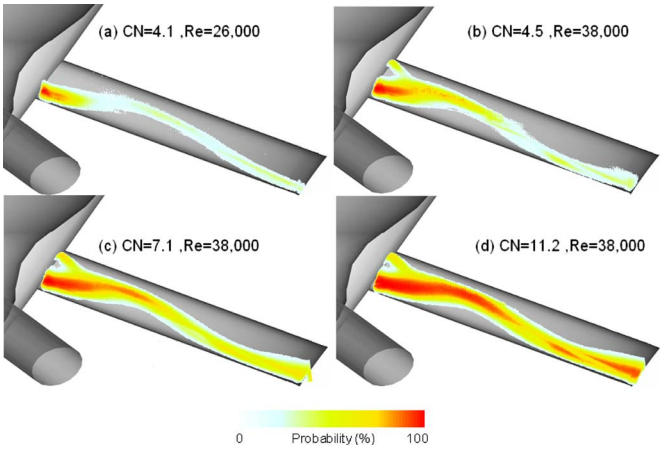


FIG. 13. (Color online) Effect of Reynolds and CNs on spatial probability of string cavitation location (needle lift: $0.3\times10^{-3}$ m).

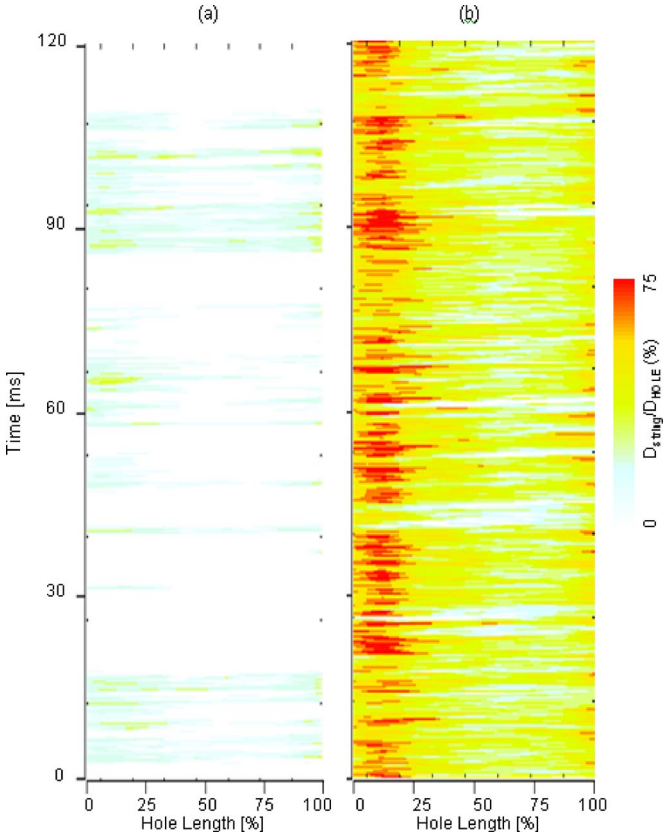


FIG. 14. (Color online) Effect of needle lift on spatial extent and temporal development of string cavitation inside the injection. (a) Needle lift: $1.5\times10^{-3}$ m, Re=66 000, and CN≈11 and (b) needle lift: $0.3\times10^{-3}$ m, Re =38 000, and CN≈11; color according to normalized string diameter.

distribution inside the nozzle. As a result, lesser cavitation strings have been observed; this can be seen by inspecting the instantaneous string appearance and size of Fig. 14. For comparison, the corresponding image obtained at the same CN but for the low needle lift case is also replotted here.

Figure 15 shows the comparison between the two needle lift cases on the percentage time of string appearance for the highest CN. Increasing needle lift results to a gradual drop in the string appearance until they eventually disappear at the highest needle lift case investigated. Their size is also reduced to more than half compared to the lowest needle lift case. This reduction is more profound at the hole inlet; as it can be seen, at this intermediate needle lift case the average

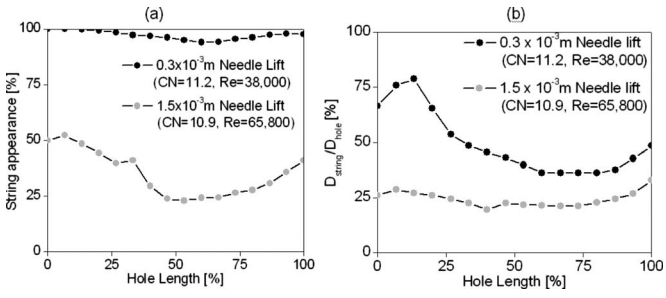


FIG. 15. Effect of the needle lift on (a) string appearance along the hole length expressed as percentage of time and (b) normalized mean string diameter along the hole length.

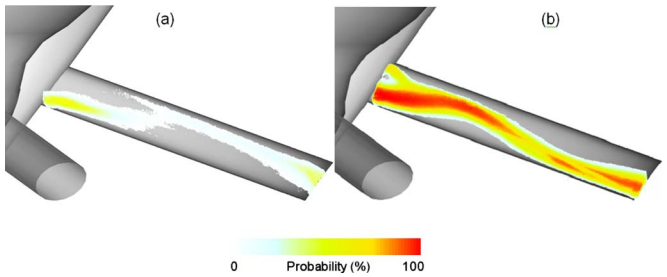


FIG. 16. (Color online) Effect of needle lift on spatial probability of string cavitation location. (a) Needle lift: $1.5\times10^{-3}$ m, Re=66 000, and CN ≈11 and (b) needle lift: $1.5\times10^{-3}$ m, Re=38 000, and CN≈11.

string diameter remains almost constant along the injection hole with an increasing trend toward the hole exit. Finally, Fig. 16 indicates that some differences can be also appreciated in the probability of finding string cavitation at a specific location inside the injection hole. Strings now are occupying the upper surface of the injection hole toward its exit but they are still concentrated at the lower part at its inlet.

Closing, it has been considered useful to summarize the various findings of the observed flow regimes in flow maps that can be reconstructed by temporal and spatial averaging the instantaneous hole cavitation images at a specific operation point. Such averages are performed from every operating point and the corresponding results are shown in the contour plot of Fig. 17. The two axes selected for plotting the results are the CN and the needle lift since these two are the most influential parameters. The contour levels represent normalized averages of the percentage hole area occupied by cavitation; from the previous results this parameter is expected to take values up to 50%. This is realized at low needle lifts and increased CN. The cavitation inception number, of around 2, can be realized from these plots. Fully developed cavitation is realized for CNs above 5 as the horizontal shape of the plotted lines indicate.

## IV. CONCLUSIONS

High speed visualization of the cavitation structures forming in enlarged tapered Diesel VCO nozzle designs has been reported, addressing questions for their origin, area of formation, size, and lifetime. Interpretation of the obtained images has been assisted by CFD predictions of the nozzle and hole flow. The specific designs tested incorporate six

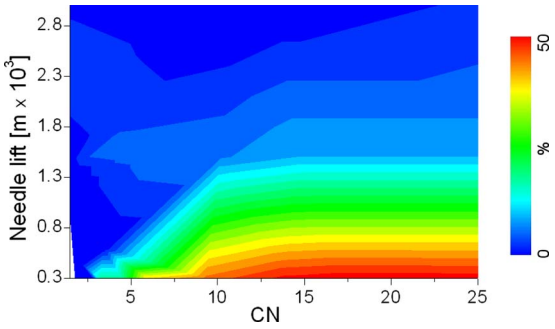


FIG. 17. (Color online) Flow map showing the normalized percentage hole area occupied by string cavitation as function of needle lift and CN.

cylindrical as well as tapered holes; tests were performed at fixed flow rate and needle lift positions. Cavitation images have revealed that although the conical shape of the converging tapered holes suppresses formation of geometric cavitation, known to form at the entry to the cylindrical injection hole, string cavitation has been found to prevail, particularly at low needle lifts. Cavitation strings appear in areas where large-scale vortices develop and originate either from preexisting geometric-induced cavitation sites or even from trapped air, present downstream of the hole exit. Computational fluid dynamics simulations have shown that these vortical structures, which act as the tracers of cavitation strings are mainly formed upstream of the injection holes due to the nonuniform flow distribution upstream of the injection holes and persist also inside the injection hole. Cavitation strings have been frequently observed to link adjacent holes. The nozzle flow and cavitation strings have been found to be sensitive to small variations in the needle shape upstream of the injection holes as well as to needle eccentricity. The effect of Reynolds and CNs on their temporal and spatial development has been examined. Processing of the acquired images has allowed estimation of the probability of finding cavitation strings at a specific location in the space between adjacent holes as well as inside them. Information for their frequency of formation, time of development, frequency of appearance and size within the injection hole has been also reported.

## ACKNOWLEDGMENTS

The authors would like to thank Dr. J. M. Nouri and Professor C. Arcoumanis for providing the experimental rig and test facilities at City University London used in the present investigation.

[1] C.-T. Hsiao and G. Chahine, "Numerical study of cavitation inception due to vortex/vortex interaction in a ducted propulsor," 25th Symposium on Naval Hydrodynamics, 2004 [J. Ship Res. **52**, 114 (2008)].
[2] R. E. A. Arndt, "Cavitation if fluid machinery and hydraulic structures," Annu. Rev. Fluid Mech. **13**, 273 (1981).
[3] R. E. A. Arndt, "An experimental insight into the effect of confinement on tip vortex cavitation of an elliptical hydrofoil," J. Fluid Mech. **290**, 1 (1999).
[4] C.-T. Hsiao and L. L. Pauley, "Numerical study of the steady-state tip vortex flow over a finite-span hydrofoil," ASME J. Fluids Eng. **120**, 345 (1998).
[5] C. E. Brennen, *Cavitation and Bubble Dynamics* (Oxford University Press, New York, 1995).
[6] R. E. A. Arndt, "Cavitation in vortical flows," Annu. Rev. Fluid Mech. **34**, 143 (2002).
[7] A. Andriotis, M. Gavaises, and C. Arcoumanis, "Vortex flow and cavitation in Diesel injector nozzles," J. Fluid Mech. **610**, 195 (2008).
[8] G. K. Batchelor, *An Introduction to Fluid Dynamics* (Cambridge Publications, Cambridge, 1967).
[9] P. G. Saffman, *Vortex Dynamics* (Cambridge Publications, Cambridge, 1992).
[10] H. Chaves, M. Knapp, A. Kubitzek, and F. Obermeier, "Experimental study of cavitation in the nozzle hole of Diesel injectors using transparent nozzles," SAE Paper No. 950290 (1995).
[11] C. Badock, R. Wirth, A. Fath, and A. Leipertz, "Investigation of cavitation in real size Diesel injection nozzles," Int. J. Heat Fluid Flow **20**, 538 (1999).
[12] C. Arcoumanis, M. Badami, H. Flora, and M. Gavaises, "Cavitation in real-size multi-hole Diesel injector nozzles," SAE Paper No. 2000-01-1249 (2000).
[13] C. Soteriou, M. Smith, and R. J. Andrews, "Cavitation hydraulic flip and atomization in direct injection Diesel sprays," IMechE Paper No. C465/051/93 (1993).
[14] C. Soteriou, R. J. Andrews, and M. Smith, "Direct injection Diesel sprays and the effect of cavitation and hydraulic flip on atomization," SAE Paper No. 950080 (1995).
[15] L. He and F. Ruiz, "Effect of cavitation on flow and turbulence in plain orifices for high-speed atomization," Atomization Sprays **5**, 569 (1995).
[16] J. H. Kim, K. Nishida, and H. Hiroyasu, "Characteristics of internal flow in a Diesel injection nozzle," International Journal of Fluid Mechanics Research **24**, 34 (1997).
[17] M. Blessing, G. König, C. Krüger, U. Michels, and V. Schwarz, "Analysis of flow and cavitation phenomena in Diesel injection nozzles and its effect on spray and mixture formation," SAE Paper No. 2003-01-1358 (2003).
[18] H. Afzal, C. Arcoumanis, M. Gavaises, and N. Kampanis, "Internal flow in Diesel injector nozzles: Modelling and experiments," IMechE Paper No. S492/S2/99 (1999).
[19] C. Arcoumanis, M. Gavaises, J. M. Nouri, E. Abdul-Wahab, and R. W. Horrocks, "Analysis of the flow in the nozzle of a vertical multi hole Diesel engine injector," SAE Transactions Journal of Engines **107**, 980811 (1998).
[20] H. Roth, M. Gavaises, and C. Arcoumanis, "Cavitation initiation: Its development and link with flow turbulence in Diesel injector nozzles," SAE Paper No. 2002-01-0214 (2002).
[21] J. Jeong and F. Hussain, "On the identification of a vortex," J. Fluid Mech. **285**, 69 (1995).
[22] M. Gavaises and A. Andriotis, "Cavitation inside multi-hole injectors for large Diesel engines and its effect on the near-nozzle spray structure," SAE Paper No. 2006-01-1114 (2006).
[23] J. M. Nouri, N. Mitroglou, Y. Y. Yan, and C. Arcoumanis, "Internal flow and cavitation in a multi-hole injector for gasoline direct-injection engines," SAE Paper No. 2007-01-1405 (2007).
[24] C. Soteriou, M. Smith, and R. J. Andrews, "Diesel injection: Laser light sheet illumination of the development of cavitation in orifices," IMechE Paper No. C529/018/98 (1998).
[25] E. Giannadakis, D. Papoulias, M. Gavaises, C. Arcoumanis, C. Soteriou, and W. Tang, "Evaluation of the predictive capability of Diesel nozzle cavitation models," SAE Paper No. 2007-01-0245 (2007).
[26] D. P. Schmidt, C. J. Rutland, and M. L. Corradini, "A fully compressible, two-dimensional model of small, high-speed, cavitating nozzles," Atomization Sprays **9**, 255 (1999).
[27] A. K. Singhal, M. M. Athavale, H. Y. Li, and Y. Jiang, "Mathematical basis and validation of the full cavitation model," ASME Trans. J. Fluids Eng. **124**, 617 (2002).
[28] E. Giannadakis, "Modelling of cavitation in automotive fuel injector nozzles," Ph.D. thesis, Imperial College, University of London, 2005.
[29] M. Gavaises, D. Papoulias, A. Andriotis, E. Giannadakis, and A. Theodorakakos, "Link between cavitation development and erosion damage if Diesel fuel injector nozzles," SAE Paper No. 2007-01-0246 (2007).
[30] E. Giannadakis, M. Gavaises, and C. Arcoumanis, "Modelling cavitation in Diesel injector nozzle holes," J. Fluid Mech. **616**, 153 (2008).
[31] E. Giannadakis, D. Papoulias, A. Theodorakakos, and M. Gavaises, "Simulation of cavitation in outwards opening pintle injectors," Proc. Inst. Mech. Eng., Part D (J. Automob. Eng.) **222**, 1895 (2008).
[32] C. Arcoumanis, H. Flora, M. Gavaises, N. Kampanis, and R. Horrocks, "Investigation of cavitation in a vertical multi-hole injector," SAE Paper No. 1999-01-0524 (1999).
[33] H. Roth, E. Giannadakis, M. Gavaises, C. Arcoumanis, K. Omae, I. Sakata, M. Nakamura, and H. Yanagihara, "Effect of multi-injection strategy on cavitation development in Diesel injector nozzle holes," SAE Paper No. 2005-02-1237 (2005).
[34] A. Andriotis and M. Gavaises, "Influence of vortex flow and cavitation on Near-nozzle Diesel spray dispersion angle," Atomization Sprays **19**, 247 (2009).
[35] A. Andriotis, M. Spathopoulou, and M. Gavaises, "Effect of nozzle flow and cavitation structures on spray development in low-speed two-stroke Diesel engines," *Proceedings 25th CIMAC World Congress on Combustion Engine Technology*, 21–24 May 2007 (International Council on Combustion Engines CIMAC, Frankfurt, 2007).